OPEN

Uncovering Vulnerable Phases in Cochlear Implant Electrode Array Insertion: Insights from an In Vitro Model

*†Philipp Aebischer, †Stefan Weder, †Mattheus Vischer, †Georgios Mantokoudis, *†Marco Caversaccio, and †‡Wilhelm Wimmer

**ARTORG Center for Biomedical Engineering, University of Bern, Switzerland; †Department for Otolaryngology, Head and Neck Surgery, Inselspital University Hospital Bern, Switzerland; and ‡Technical University of Munich, Germany; TUM School of Medicine, Klinikum rechts der Isar, Department of Otorhinolaryngology*

Objectives: The aim of this study is to improve our understanding of the mechanics involved in the insertion of lateral wall cochlear implant electrode arrays.
Design: A series of 30 insertion experiments were conducted by three experienced surgeons. The experiments were carried out in a previously validated artificial temporal bone model according to established soft surgery guidelines. The use of an in vitro setup enabled us to comprehensively evaluate relevant parameters, such as insertion force, intracochlear pressure, and exact electrode array position in a controlled and repeatable environment.
Results: Our findings reveal that strong intracochlear pressure transients are more frequently caused during the second half of the insertion, and that regrasping the electrode array is a significant factor in this phenomenon. For choosing an optimal insertion speed, we show that it is crucial to balance slow movement to limit intracochlear stress with short duration to limit tremor-induced pressure spikes, challenging the common assumption that a slower insertion is inherently better. Furthermore, we found that intracochlear stress is affected by the order of execution of post-insertion steps, namely sealing the round window and posterior tympanotomy with autologous tissue and routing of the excess cable into the mastoid cavity. Finally, surgeons' subjective estimates of physical parameters such as speed, smoothness, and resistance did not correlate with objectively assessed measures, highlighting that a thorough understanding of intracochlear mechanics is essential for an atraumatic implantation.
Conclusion: The results presented in this article allow us to formulate evidence-based surgical recommendations that may ultimately help to improve surgical outcome and hearing preservation in cochlear implant patients.
Key Words: Cochlear implantation—Insertion mechanics—Soft surgery.

Otol Neurotol **00:**00–00, 2024.

INTRODUCTION

Cochlear implants (CIs) are widely used to treat severe-to-profound sensorineural hearing loss. The insertion of the electrode array through the round window is a crucial surgical step that requires precision and care. While both implants and surgical techniques have undergone significant improvements over the years to minimize trauma during this phase, the surgeon's hand movement is still directly transmitted to the scala tympani. Consequently, the risk of intracochlear trauma remains a concern, with tremor and micromovements shown to produce intracochlear pressure levels that may result in permanent damage to the delicate inner ear structures (1). In recent years, inclusion criteria have expanded to include patients with residual hearing, for which preservation of intracochlear structures is essential. Thus, identifying the vulnerable phases of cochlear implant electrode array insertion is critical to improving surgical outcome and reducing the risk of complications.

The cochlea is situated deep within the temporal bone, and the structures of the auditory organ are too small to be visualized accurately using medical imaging techniques in patients (2,3). This poses a significant challenge since there are limited means available to analyze insertion-related intracochlear processes. Several methods were developed to objectify cochlear implantation, including the utilization of fluoroscopy (4), ECochG, and impedance telemetry, which can aid in estimating implant position (5–11) and identifying traumatic events (12–14). Additionally, cadaveric specimens have been employed to measure intracochlear pressure and insertion forces (1,15,16). However, despite these efforts, it remains difficult to establish

Address correspondence and reprint requests to Philipp Aebischer, Ph.D., Murtenstrasse 50, 3008 Bern, Switzerland; E-mail: philipp.aebischer@unibe.ch

Financial disclosures/conflicts of interest: There are no conflicts of interest, financial, or otherwise.

DOI: 10.1097/MAO.0000000000004130

clear relationships between treatment outcomes and the insertion-related factors that influence them.

Given the limited opportunities for measuring intracochlear processes in patients and cadaveric specimens, in vitro models can provide complementary features for analysis. These models allow for precise visualization of the electrode array within the cochlea, along with synchronous high-resolution sensory monitoring.

Therefore, in this study, we aim to comprehensively monitor intracochlear pressure, insertion forces, and electrode array movement during the phases of electrode array insertion and implant management using an artificial model of the temporal bone that replicates the 3D geometry of the scala tympani and incorporates realistic friction characteristics (17,18). Our objective is to deepen our understanding of the factors that may contribute to inner ear injury during the implantation process. Ultimately, we hope to provide a more complete picture of cochlear implantation that can inform the development of safer and more effective surgical techniques.

METHODS

Study Protocol

For this study, three experienced CI surgeons inserted straight electrode array dummies into an artificial temporal bone model while following the soft surgery protocol (19). The surgeons were furthermore instructed to seal the model's round window and facial recess with fascia or muscle tissue and route the electrode lead into the mastoid cavity. Porcine abdominal tissue was used to seal the round window and facial recess. Surgeons were provided access to surgical tools such as forceps, microhook, and pick and were allowed to use their preferred surgical techniques. The procedures were performed with a surgical microscope (M525; Leica Microsystems GmbH, Wetzlar, Germany). Each surgeon repeated the insertion process 10 times, resulting in a total of 30 insertions. After each insertion, speed, resistance, smoothness, tremor, and alignment were rated on a visual analog scale.

Setup

The test bench comprises a scala tympani model embedded in a full temporal bone model. The scala tympani model is a clear epoxy cast that allows for optical recording of the electrode array using a digital microscope (USB Digital Microscope, Z-Star Microelectronics Corporation). It is mounted on a load cell (KD78, ME Meßsysteme GmbH, Hennigsdorf, Germany and HX711 load cell amplifier, SparkFun Electronics, Niwot, CO) that measures the force applied along the long axis of the cochlea. Intracochlear pressure is measured at the cochlear apex using a dedicated sensor (MS5837-02BA; Measurement Specialties, Inc, Hampton, VA). The scala tympani model is embedded in a mechanically decoupled 3D-printed temporal bone model that features a mastoidectomy, posterior tympanotomy, cochlear promontory, and round window niche.

A thin, flexible film (stretched Parafilm “M” laboratory film; Bemis Company, Inc, Neenah, WI) with a punched hole (radius 0.25 mm) was placed at the entrance of the scala tympani model to mimic the soft tissue of the round window membrane. The film was verified to produce no measurable resistance during insertion of the electrode and was replaced after each iteration.

In addition, we mounted a slide potentiometer to track the opening and closing of the surgical forceps, and recorded the surgical view through the microscope using an external recorder (Storz IMAGE1 HD with TELE PACK+). The setup was previously described in full detail in a study that evaluated a novel manual insertion tool (18). Figure 1 shows the temporal bone model during an insertion as seen by the operator, together with a photomicrograph of the scala tympani model containing a partially inserted electrode array.

Scala Tympani Model

The scala tympani model reproduces the macroanatomy obtained from micro computed tomography scan of a human cochlea. The Segmentation was obtained from the HEAR-EU Multiscale Imaging and Modeling Dataset of the Human Inner Ear (dataset *D_9*) (20). The model was fabricated by 3D printing an ABS negative, manually

FIG. 1. Left: View through the surgical microscope showing the temporal bone model and mastoidectomy, and the black dummy electrode array attached to the electrode lead of the implant body. Right: Photomicrograph of the scala tympani model of the same insertion, showing the partially inserted array. A small air gap (0.5 mm) decouples the scala tympani model mechanically, allowing to measure insertion forces unaffected by the promontory.

improving the surface quality, casting it in clear epoxy resin and leaching out the internal ABS model. To reproduce realistic frictional properties, the model is coated with a polymer brush coating (graft co-polymer with a poly(L-lysine) backbone and poly(ethylene glycol) side-chains, PEG-g-PLL), rendering the surface hydrophilic, analoguous to the endosteum covering the cochlear walls. We describe the full fabrication and coating process as well as the validation of insertion forces for cochlear implant insertion in a technical note (17).

Electrode Array Dummies

We used dummy electrode arrays that mirror bending stiffness and exact geometry of the MedEl Flex28 electrode array (MED- EL GmbH, Innsbruck, Austria). This array was chosen as it is the most implanted type at our institution. The dummies were glued to the electrode lead of a cochlear implant body (Synchrony, MED-EL). Dummies are colored black to allow optical centerline detection from photomicrographs of the scala tympani model. Full details on fabrication of these electrode array dummies was also provided in (17).

Outcome Measures

We simultaneously recorded the applied force, the intracochlear pressure, the forceps opening width, a video capture of the surgical microscope, and a microscope video capture of the cochlear basal plane. An estimation of the electrode centerline was automatically computed from the latter using a previously described method (21). The centerline enabled us to calculate secondary metrics such as linear and angular insertion depth (the length of the centerline starting at the round window, and the azimuth of the polar coordinates, respectively), insertion speed (the time derivative of the linear insertion depth), and the transverse position of the electrode array relative to the scala tympani centerline at an intracochlear position of 90° (18).

Work Midpoint

The integral of the applied force as a function of the insertion depth yields the total energy required to insert the electrode array, called the *insertion work* (18). To aid in our analysis, we defined a new metric, called the *work midpoint*, which corresponds to the point where the preceding and succeeding divisions of the insertion require equal amounts of work.

Force Variation, Pressure Variation, and Transverse Electrode Movement

We defined the *variation* of a quantity as the standard deviation of the measured signal over time. To obtain the distribution of the variation over the full insertion process, we divided the signal into segments of 5 seconds and computed the histogram of the variation of these segments.

Insertion Speed

To compare slow and fast phases of the insertion, the *speed* at a specific time point was defined as the average speed value across a centered window with a window width of 10 seconds.

Contributor Separation in Outcome Measures

We observed that the sequence of steps performed after the implant insertion impacted several metrics. As this order of execution was also associated with the individual surgeon performing the procedure, we conducted a two-way ANOVA to assess the respective contributions of both factors. Force variation, pressure variation or transverse electrode movement respectively was set as the dependent variable, and fitted with the categorical predictor variables *order of execution* and *surgeon id*. For the purpose of this analysis, force variation, pressure variation and transverse electrode movement underwent a logarithmic transformation. Statistical analysis was performed with the statsmodels Python module, using a significance level of $\alpha = 0.05$.

RESULTS

Insertion Depth

All electrode arrays were successfully placed. The mean angular insertion depth was 626 ° ± 29° (mean ± standard deviation).

Insertion Speed

The average insertion time was 145 seconds, corresponding to an average insertion speed of 0.19 mm/s. We observed a tendency toward slower speeds near the end of the insertion. Insertion depths versus time are shown in Figure 2, together with a histogram of observed insertion speeds.

Insertion Force

Insertion forces reached a maximum level of 48 ± 12 mN. The force progression of one exemplary insertion and of the distribution of maximal forces is shown in Figure 3. The work midpoint occurred at 23.1 ± 1.0 mm and is indicated in the same figure.

Human Kinematics

Small pressure peaks occurred uniformly throughout the insertion process. Stronger pressure peaks that are likely to traumatize intracochlear structures (e.g., larger than 1 hPa) (1) were comparatively rare, and did occur mainly in the second half of the insertion. Along with this, we observed an increased occurrence of regripping of the electrode array in the second half of the procedure. The relative distribution of pressure peaks grouped by peak height is shown in the center row of Figure 4, and a histogram of the occurrence of regripping in the top row of the same figure.

Releasing the electrode was often associated with intracochlear movement of the array and accompanied by substantial changes in the measured force and pressure. This relation is clearly observable even in individual recordings, as is illustrated in Figure 5. Figure 6 statistically compares force variation and transverse electrode movement between moments where the electrode is firmly gripped versus during regrasping events. Regrasping lead to a significant increase in these metrics and thus to an increased level of cochlear stress.

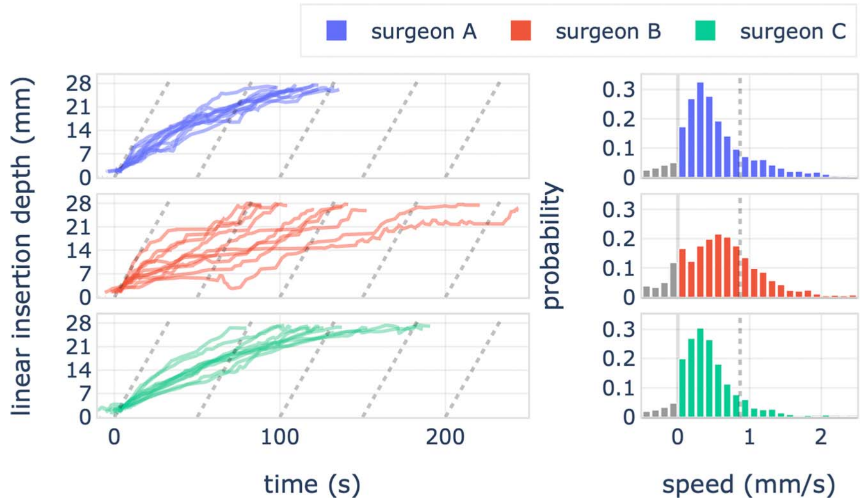

FIG. 2. Left: Linear insertion depth versus time for each surgeon. Right: Histogram of the insertion speed normalized by distance traveled. Dashed lines represent an insertion speed of 0.87 mm, identified by Kesler et al. as the lower limit of a human operator (22).

Surgical Self-Assessment

After each insertion, surgeons assessed the insertion speed, resistance, smoothness, tremor, and alignment in a questionnaire. Neither of these subjective measures were correlated with objectively measured metrics such as the force progression or maximal force, number or amplitude of pressure peaks, insertion speed or variation thereof, transverse intracochlear electrode movement or electrode alignment in the basal section of the scala tympani.

Postinsertion Management

Postinsertion management included (1) the sealing of the round window and facial recess with facia and muscle tissue and (2) the coiling of the excess electrode lead into the mastoidectomy. These steps were observed in either order, with one surgeon always starting with the coiling, one predominantly so (9 of 10 insertions), and one starting predominantly with the placement of tissue (8 of 10 cases). The cable was routed similarly in all procedures. From the round window, the cable passed in a loop through the inferior part of the mastoid cavity, resting superficially against the lip of the mastoidectomy and then continuing to the main body of the implant. Insertions that proceeded with sealing of the round window and facial recess before continuing to routing the excess electrode cable showed lower force (−3.56 mN) and pressure variations (−0.16 hPa), as well as transverse

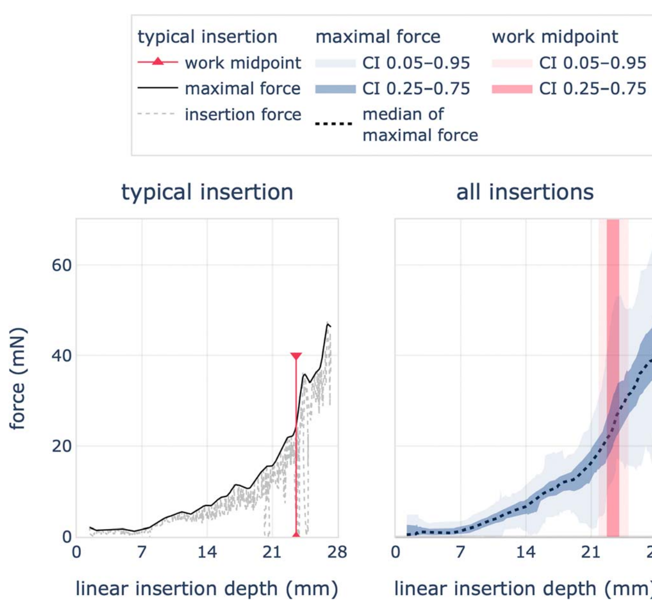

FIG. 3. Left: Insertion force and maximal force (1 mm moving window) of one insertion. The work midpoint, that splits the insertion into two segments of equal work, is marked with a red vertical line. Right: Median and confidence intervals of the maximal force of all insertions. The vertical red bar indicates the confidence intervals of the work midpoint.

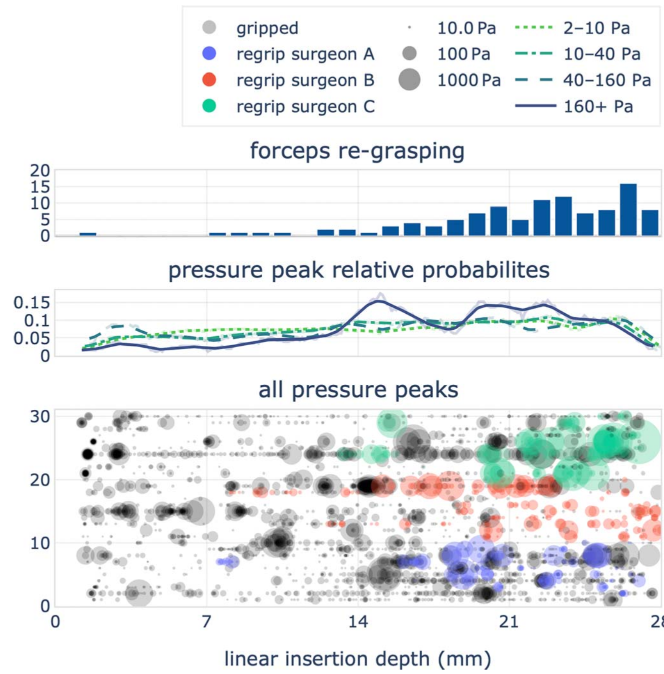

FIG. 4. Top: Regripping of the electrode array is very rare in the first half of the insertion and becomes increasingly frequent toward the end. Center: Relative probability of pressure peaks grouped by peak strength. Strong peaks occur mostly in the second half of the insertion. Bottom: Pressure peaks as a function of insertion depth of the array. Colored markers indicate pressure peaks occurring in temporal relation with the regripping of the electrode.

electrode movement (−0.026 mm). The standard deviation of these metrics during postinsertion management, categorized by order of execution, is shown in Figure 7.

The ANOVA revealed a statistically significant impact of the order of execution on force variation ($p < 0.01$), pressure variation ($p < 0.01$), and transverse electrode movement ($p = 0.03$). Conversely, the identity of the surgeon perfoming the insertion did not emerge as a predictive factor for either force variation, pressure variation or transverse electrode movement ($p = 0.62$, $p = 0.23$, and $p = 0.63$, respectively).

DISCUSSION

Surgical Self-Assessment

Surprisingly, we observed no significant correlation between the subjective self-assessment (speed, resistance,

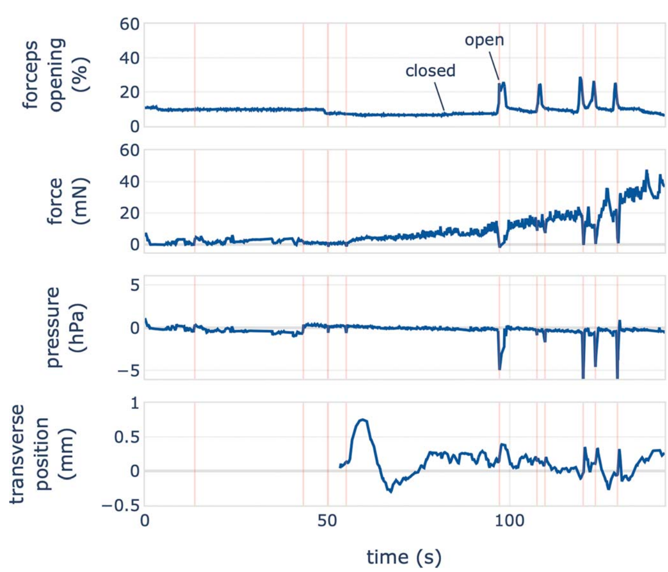

FIG. 5. Forceps pinch state, insertion force, intracochlear pressure, and transverse electrode position of one insertion. A clear correlation between these parameters is apparent.

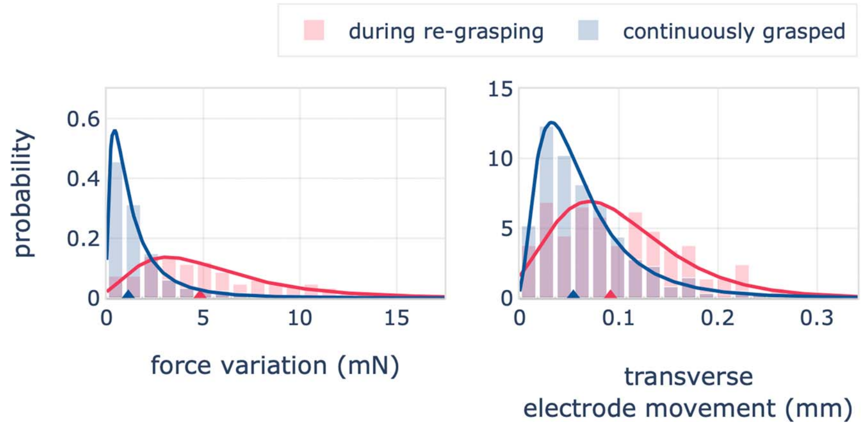

FIG. 6. Histogram of force variation (left) and intracochlear transverse electrode movement (right) during the insertion, classified by the forceps pinching state. Releasing the array is associated with significantly larger force variation and intracochlear electrode movement.

smoothness, tremor and alignment) and the corresponding objectively recorded metrics. This suggests that surgeons may face difficulties in reliably judging the procedure's physical impact on intracochlear structures. A thorough understanding of the insertion mechanics is thus indispensable for accomplishing atraumatic insertions.

Insertion Force and Work

The magnitudes of the forces exerted during the final stages of the insertion process are capable of damaging structures such as the basilar membrane and the osseous spiral lamina (21,23,24).

Our measurements indicate that insertion forces scale roughly exponentially with the insertion depth, consistent with the results of previous research (21,25). This means that a disproportionately large fraction of the cochlear stress occurs in the last millimeters of the insertion. The steep force increase deserves mention, and is well illustrated by the work midpoint. This point indicates the insertion depth at which the preceding and succeeding divisions of the insertion both require the same work. The work midpoint is plotted in Figure 3 and occurs at 23.1 mm ± 1.0 mm, only 5 mm short of the full insertion. From personal exchange with surgeons, it appears that this point is perceived to occur surprisingly late.

One factor that contributes to this misperception is that much of the insertion takes place below the surgeon's force perception threshold (26), making it impossible to correctly perceive the true ratio between early and late insertion forces. Moreover, the total force exerted on the lateral wall of the cochlea is approximately 10 times greater than the force perceived by the surgeon. This is attributed to the cochlea's coiled shape, which results in most internal forces being counterbalanced by opposing forces on the opposite lateral wall (21). Consequently, particular vigilance should be exercised toward the end of the insertion process.

Human Kinematics and Surgical Technique

We found that regripping of the electrode array is a major contributor to causing strong pressure spikes that are likely

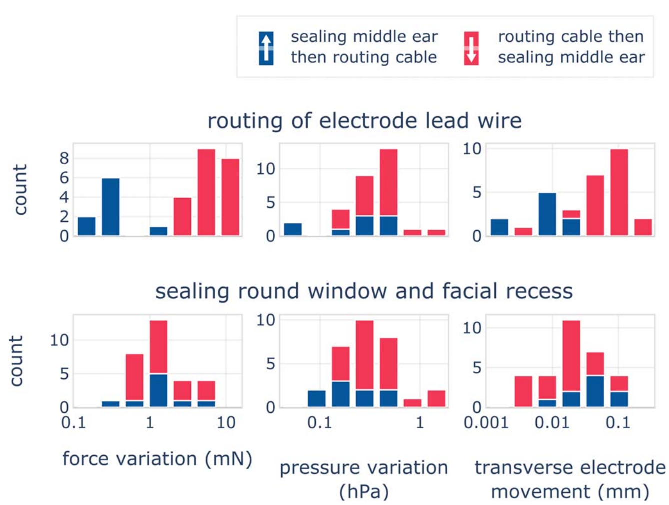

FIG. 7. Standard deviation of three different metrics during packing of the round window and facial recess and coiling of the electrode lead, classified by the execution order of these two steps. Left: Force variation. Center: Pressure variation. Right: Transverse electrode movement in the basal portion of the scala tympani.

to traumatize intracochlear structures. This suggests that regripping of the electrode array should be minimized during the surgical procedure. In addition, methods for stabilizing the array are advisable. Surgeon *A* stabilized the array with a microhook at the inferior margin of the facial recess. Surgeon *B* secured the proximal portion of the cable between the index finger and thumb, rested on the temporal bone. Both approaches appear to contribute to lower and fewer pressure peaks (see Fig. 4, bottom).

Insertion Speed

Kesler et al. determined a lower limit of 0.87 mm/s for a continuous forward insertion in manual cochlear implantation (22). Our measurements show that surgeons can move the electrode array at significantly lower speeds. In contrast to their setup, ours includes a full temporal bone model, and instead of tracking the forceps we directly measured the speed of the array. In evaluating the video material, we found that our surgeons used to rest fingers directly on the mastoid surface, which might help to stabilize the hand and improve dexterity. It is also worth noting that surgeon *A* requested verbal signaling of the passing of 15 second increments and achieved very steady insertions (c.f., Fig. 2, first row).

In a retrospective analysis of 40 clinical insertions, Rajan et al. found a higher rate of complete insertions when inserting the electrodes slowly. They hypothesized that slow insertions allow for better pressure equilibration and thus reduce intracochlear pressure peaks (27). However, we did observe only a negligible correlation between the momentary speed of the array and corresponding intracochlear pressure peaks (Pearson's $r = 0.12$, $p < 0.001$). Steady or slow portions of the insertions did not lead to lower or fewer pressure peaks.

Furthermore, contrary to findings in continuously driven, motorized experiments (21,28,29), we did not observe any relevant correlation between the insertion speed and the average force, maximal force or force variation.

According to our results, the primary contributor to pressure peaks, transverse electrode movement, and force variation is not the overall speed of insertion, but rather small variations therein. These variations can result from tremor and, more importantly, the release and regripping of the electrode array. Hence, the notion widely held that intracochlear trauma can be mitigated by slow insertions may oversimplify the issue. Our results suggest that a balance must be achieved, since the benefit of decreasing stress by slowing down the insertion rate shows little benefit for speeds typical for a soft surgery approach and comes at the cost of increased exposure to pressure spikes caused by electrode micromovements.

Postinsertion Management

Soft surgery recommendations usually focus on opening the cochlea and inserting the electrode array (30). Our measurements indicate that electrode management after these steps can still have a substantial impact on intracochlear pressure and electrode movement. Insertions that proceeded with sealing of the round window and facial recess before continuing to routing the excess electrode cable showed substantially lower force and pressure variations, as well as transverse electrode movement.

Note that these results should be interpreted conservatively, as the order of execution was a personal preference of the surgeon, and general intersubject differences may amplify the effect. However, for the two surgeons who performed procedures in both orders, the trend remains observable even when only intrasubject variation is considered. Accounting for mutual influence of the order of execution and surgeon id using an ANOVA, we observed a statistically significant impact of the order on postinsertion force variation, pressure variation and transverse electrode movement, while no such relation emerged for the surgeon performing the insertion. Nonetheless, given the strong preference of individual surgeons for a particular order and the inhomogeneous distribution of data, further testing in this regard should be performed.

An additional way to address postinsertion electrode movement would be to fix the electrode lead immediately after the insertion, for example in a bone groove drilled into the inferior margin of the facial recess (31).

Links to Other Research

ECochG is a widely used tool for assessing cochlear health during electrode insertion. Amplitude drops have been reported to occur at any time during the insertion process, and this behavior may be related to the present findings (32). Intracochlear electrode movement caused by regripping can alter the electrode's contact with the basilar membrane, affecting the mechanics of acoustic stimulation and, consequently, ECochG measurements (33). In addition, exposure to loud noises and associated pressure peaks can cause temporary hearing threshold shifts by disrupting synaptic connections, impairing mechanoelectrical transduction channels of the hair cells, and inducing morphological changes in the tectorial membrane (34). These threshold shifts are likely to further influence ECochG outcomes. Depending on their severity, hearing thresholds can recover within minutes, which may explain the variable and fluctuating nature of ECochG recordings. The late occurrence of the work midpoint is also consistent with the timing of ECochG events, which occur most frequently in the last stages of the electrode insertion (35,36).

ECochG signal drops during placement of fascia and placement of the electrode array within the mastoid cavity have also been well documented (35,37) and are a recurring concern in clinical routine (38). This agrees with our results, which revealed that postinsertion surgical steps regularly cause intracochlear movement of the electrode array, which is expected to impact ECochG.

One approach to mitigate pressure peaks during electrode insertion is to use a motorized tool (39). Nonconstant, decreasing insertion speeds can be used to minimize maximum forces and favorably adjust the work midpoint (21). Current systems are used in conjunction with a conventional surgical approach (40,41), thus our findings regarding postinsertion implant management apply to them as well. Consequently, it is important that care is taken when detaching the electrode array from the tool's holding mechanism. These systems effectively minimize micromovements of the electrode array, but still operate within anatomic constraints, resulting in comparable insertion forces (21). Alternatively, the electrode array can be stabilized during insertion using a guide tube (42) or a manual insertion tool previously developed at our institution. This tool deflects the electrode array intracochlearly, allowing further reduction of maximum forces (18).

Evidence-Based Surgical Recommendations

Particular care must be taken in the last phase of the electrode array insertion, since exponentially increasing forces imply that a large part of the total insertion energy is applied in a short period of time. Therefore, it is advised to avoid regrasping and focus on steady and slow movement during this phase. This is especially important, as surgeons may underestimate this effect because early force levels are well below the perception threshold, which means that the true force increase is not reflected by haptic feedback.

The importance of minimizing fast electrode movements is underscored by the amplitudes of the observed pressure peaks. Such movements can be caused by tremor or by readjusting the forceps grip. To mitigate these issues, we recommend taking steps to reduce tremors and to readjust the forceps grip only when necessary. Surgeons should rest their wrist and fingers on the mastoid surface close to the surgical site and begin with a posture that allows to complete the full insertion movement. When readjusting the forceps grip, the electrode array should be adequately secured to ensure that it doesn't move excessively. To accomplish this, the proximal segment of the electrode cable can be held manually, or a microhook can be used to secure the electrode array to the inferior margin of the facial recess.

A slow insertion is important to allow perilymph equalization and to keep the insertion forces low (21,27,28). However, these findings result from continuously driven robotic experiments or fast manual insertions. Within the range of speeds of soft surgery recommendations observed herein, we did not find any benefits of slow insertions with respect to force and pressure. On the other hand, an excessively slow insertion can unnecessarily increase intracochlear exposure to tremor, which is directly coupled in via the electrode array held by the surgeon. It is worth noting that this challenges the popular notion that insertions should be carried out as slowly as possible. We believe that an insertion time around 90 seconds is a reasonable compromise that allows for pressure equalization while limiting pressure transients caused by tremor. To achieve uniform insertion speeds, a timer indicating regular intervals (e.g., every 15 seconds) can be used.

Finally, first closing the facial recess with autologous tissue before routing the excess cable into the mastoid cavity might contribute to reduce stress on the cochlea.

Study Limitations

The study protocol intentionally allowed surgeons to use their personal techniques for implant placement. This ensured that the surgeons performed their tasks in a way they were comfortable with, and we were able to observe and compare different individual preferences. The downside, however, is that it is not always possible to clearly separate all the parameters that contribute to a particular outcome.

In addition, all surgeons practice at the same hospital. Even though they learned the procedure at different institutions, their techniques may not be representative of cochlear implant surgery in general. A comparison among surgeons from different institutes could improve our understanding on which techniques are commonly employed in CI surgery.

Furthermore, the study was restricted to a single implant model in a single temporal bone model. Implants of different manufacturers do substantially differ in length and stiffness and may lead to different intracochlear behavior. Pressure transients originating from regrasping, for example, are a direct consequence of the array's elastic behavior, and it remains to be tested whether stiffer arrays lead to a decrease in pressure transients due to reduced springiness or increase due to larger restoring forces. For pressure transients originating from tremor, we expect similar results for different implants, as they are a consequence of fluid displacement due to array motion. Similarly, we expect postinsertion mechanics to be similar because of similar stiffness of the extracochlear portion of electrode lead for different manufacturers. However, these considerations are speculative and require further testing with a wider range of electrode models.

More generally, the kinematics of inserting perimodiolar arrays are very different and likely not well represented in the present study. Furthermore, anatomical variations are known to affect the intracochlear position of the electrode array and insertion forces (21), and are expected to impact the results obtained herein. Finally, our results and conclusions were found from in vitro experiments. Ultimately, their applicability and effectiveness need to be demonstrated in clinical cases. For this purpose, parameters that can be recorded in the surgical theater could be compared with postoperative hearing outcomes.

CONCLUSION

This in vitro study comprehensively investigated all phases of the electrode array insertion process in cochlear implantation. By synchronously measuring a wide range of parameters related to both biomechanical loads and operator kinematics, we obtained an understanding of the stresses imposed on the cochlea and how they are affected by surgical behavior. These data enabled us to identify the impact of different insertion phases and derive surgical recommendations.

We observed that strong intracochlear pressure peaks occur increasingly during the second half of the insertion. Many of the most substantial pressure peaks are associated with a release and regrasping of the electrode array. The intensity of these pressure peaks is likely to result in temporary or even long-term damage to the inner ear structures.

As a significant portion of the insertion process occurs below the surgeon's force perception threshold, the actual force increase cannot be accurately assessed. To address this, we introduce the concept of the work midpoint, which demonstrates that approximately half of the total insertion work is exerted over the final 5 mm of the insertion.

Within the range of insertion speeds typical of a soft surgery approach we did observe no benefits of particularly slow movements on force and pressure. An optimal insertion speed must therefore balance slow movements in accordance with soft surgery guidelines with reducing unnecessary long exposure to tremor-induced pressure spikes.

Finally, postinsertion cable management still affects the intracochlear portion of the electrode array. Its contribution seems to be minimized by using autologous tissue to stabilize the electrode array in the facial recess before routing the excess cable into the mastoidectomy.

These findings may improve our understanding of the processes contributing to inconsistent hearing outcomes in CI patients and ultimately help reduce trauma during cochlear implantation.

REFERENCES

1. Greene NT, Mattingly JK, Banakis Hartl RM, Tollin DJ, Cass SP. Intracochlear Pressure Transients During Cochlear Implant Electrode Insertion. *Otol Neurotol* 2016;37:1541–8.
2. Karkas A, Boureille P, Laroche N, et al. Imaging of the human cochlea using micro-computed tomography before and after cochlear implantation: Comparison with cone-beam computed tomography. *Eur Arch Otorhinolaryngol* 2023;280:3131–40.
3. Wimmer W, Bell B, Huth ME, et al. Cone beam and micro-computed tomography validation of manual array insertion for minimally invasive cochlear implantation. *Audiol Neurootol* 2014;19:22–30.
4. Perazzini C, Puechmaille M, Saroul N, et al. Fluoroscopy guided electrode-array insertion for cochlear implantation with straight electrode-arrays: a valuable tool in most cases. *Eur Arch Otorhinolaryngol* 2021; 278:965–75.
5. Vanpoucke FJ, Boermans PB, Frijns JH. Assessing the placement of a cochlear electrode array by multidimensional scaling. *IEEE Trans Biomed Eng* 2012;59:307–10.
6. Helmstaedter V, Lenarz T, Erfurt P, Kral A, Baumhoff P. The summating potential is a reliable marker of electrode position in electrocochleography: cochlear implant as a theragnostic probe. *Ear Hear* 2018;39:687–700.
7. de Rijk SR, Tam YC, Carlyon RP, Bance ML. Detection of extracochlear electrodes in cochlear implants with electric field imaging/transimpedance measurements: a human cadaver study. *Ear Hear* 2020;41:1196–207.
8. Bruns TL, Riojas KE, Labadie RF, Webster Iii RJ. Real-time localization of cochlear-implant electrode arrays using bipolar impedance sensing. *IEEE Trans Biomed Eng* 2022;69:718–24.
9. Aebischer P, Meyer S, Caversaccio M, Wimmer W. Intraoperative impedance-based estimation of cochlear implant electrode array insertion depth. *IEEE Trans Biomed Eng* 2021;68:545–55.
10. Schraivogel S, Aebischer P, Weder S, Caversaccio M, Wimmer W. Cochlear implant electrode impedance subcomponents as biomarker for residual hearing. *Front Neurol* 2023;14:1183116.
11. Schraivogel S, Aebischer P, Wagner F, et al. Postoperative impedance-based estimation of cochlear implant electrode insertion depth. *Ear Hear* 2023;44:1379–88.
12. Dalbert A, Pfiffner F, Hoesli M, et al. Assessment of cochlear function during cochlear implantation by extra- and intracochlear electrocochleography. *Front Neurosci* 2018;12. doi:10.3389/fnins.2018.00018.
13. Trecca EMC, Adunka OF, Mattingly JK, et al. Electrocochleography observations in a series of cochlear implant electrode tip fold-overs. *Otol Neurotol* 2021;42:e433–7.
14. Wimmer W, Sclabas L, Caversaccio M, Weder S. Cochlear implant electrode impedance as potential biomarker for residual hearing. *Front Neurol* 2022;13:886171.
15. Nguyen Y, Miroir M, Kazmitcheff G, et al. Cochlear implant insertion forces in microdissected human cochlea to evaluate a prototype array. *Audiol Neurootol* 2012;17:290–8.
16. Avci E, Nauwelaers T, Hamacher V, Kral A. Three-dimensional force profile during cochlear implantation depends on individual geometry and insertion trauma. *Ear Hear* 2017;38:e168–79.
17. Aebischer P, Caversaccio M, Wimmer W. Fabrication of human anatomy-based scala tympani models with a hydrophilic coating for cochlear implant insertion experiments. *Hear Res* 2021;404:108205.
18. Aebischer P, Weder S, Mantokoudis G, et al. A Sleeve-Based, Micromotion Avoiding, Retractable and Tear-Opening (SMART) insertion tool for cochlear implantation. *IEEE Trans Biomed Eng* 2023;70:860–6.
19. Lenarz T. Cochlear Implant - State of the Art. *Laryngorhinootologie* 2017;96(S 01):S123–51.
20. Gerber N, Reyes M, Barazzetti L, et al. A multiscale imaging and modelling dataset of the human inner ear. *Sci Data* 2017;4:170132.
21. Aebischer P, Mantokoudis G, Weder S, et al. In-vitro study of speed and alignment angle in cochlear implant electrode array insertions. *IEEE Trans Biomed Eng* 2022;69:129–37.
22. Kesler K, Dillon NP, Fichera L, Labadie RF. Human kinematics of cochlear implant surgery: an investigation of insertion micro-motions and speed limitations. *Otolaryngol Head Neck Surg* 2017;157:493–8.
23. Ishii T, Takayama M, Takahashi Y. Mechanical properties of human round window, basilar and reissner's membranes. *Acta Otolaryngol Suppl* 1995;519:78–82.
24. Mirsalehi M, Rau TS, Harbach L, et al. Insertion forces and intracochlear trauma in temporal bone specimens implanted with a straight atraumatic electrode array. *Eur Arch Otorhinolaryngol* 2017; 274:2131–40.
25. Kobler JP, Dhanasingh A, Kiran R, Jolly C, Ortmaier T. Cochlear dummy electrodes for insertion training and research purposes: fabrication, mechanical characterization, and experimental validation. *Biomed Res Int* 2015;2015:1–9.
26. Kratchman LB, Schuster D, Dietrich MS, Labadie RF. Force perception thresholds in cochlear implantation surgery. *Audiol Neurootol* 2016;21:244–9.
27. Rajan GP, Kontorinis G, Kuthubutheen J. The effects of insertion speed on inner ear function during cochlear implantation: a comparison study. *Audiol Neurootol* 2013;18:17–22.
28. Hügl S, Rülander K, Lenarz T, Majdani O, Rau TS. Investigation of ultra-low insertion speeds in an inelastic artificial cochlear model using custom-made cochlear implant electrodes. *Eur Arch Otorhinolaryngol* 2018;275:2947–56.
29. Kaufmann CR, Henslee AM, Claussen A, Hansen MR. Evaluation of insertion forces and cochlea trauma following robotics-assisted cochlear implant electrode array insertion. *Otol Neurotol* 2020;41:631–638.
30. Friedland DR, Runge-Samuelson C. Soft cochlear implantation: rationale for the surgical approach. *Trends Amplif* 2009;13:124–38.
31. Loth AG, Adel Y, Weiß R, et al. Evaluation of a bone groove geometry for fixation of a cochlear implant electrode. *Eur Arch Otorhinolaryngol* 2020;277:385–92.
32. Weder S, Bester C, Collins A, et al. Real time monitoring during cochlear implantation: increasing the accuracy of predicting residual hearing outcomes. *Otol Neurotol* 2021;42:e1030–6.
33. Bester C, Dalbert A, Collins A, et al. Electrocochleographic patterns predicting increased impedances and hearing loss after cochlear implantation. *Ear Hear* 2023;44:710–20.
34. Patuzzi R. Exponential onset and recovery of temporary threshold shift after loud sound: evidence for long-term inactivation of mechano-electrical transduction channels. *Hear Res* 1998;125(1–2):17–38.
35. Weder S, Bester C, Collins A, et al. Toward a better understanding of electrocochleography: analysis of real-time recordings. *Ear Hear* 2020;41:1560–7.
36. Campbell L, Kaicer A, Sly D, et al. Intraoperative real-time cochlear response telemetry predicts hearing preservation in cochlear implantation. *Otol Neurotol* 2016;37:332–8.

37. Harris MS, Riggs WJ, Koka K, et al. Real-time intracochlear electrocochleography obtained directly through a cochlear implant. *Otol Neurotol* 2017;38:e107–13.
38. Schuerch K, Waser M, Mantokoudis G, et al. Increasing the reliability of real-time electrocochleography during cochlear implantation: a standardized guideline. *Eur Arch Otorhinolaryngol* 2022;279:4655–65.
39. Banakis Hartl RM, Kaufmann C, Hansen MR, Tollin DJ. Intracochlear pressure transients during cochlear implant electrode insertion: effect of micro-mechanical control on limiting pressure trauma. *Otol Neurotol* 2019;40:736–44.
40. Gantz JA, Gantz BJ, Kaufmann CR, et al. A steadier hand: the first human clinical trial of a single-use robotic-assisted surgical device for cochlear implant electrode array insertion. *Otol Neurotol* 2023;44:34–9.
41. Daoudi H, Lahlou G, Torres R, et al. Robot-assisted cochlear implant electrode array insertion in adults: a comparative study with manual insertion. *Otol Neurotol* 2021;42:e438–44.
42. Wimmer W, Gavaghan K, Williamson T, et al. Electrode array insertion for minimally invasive robotic cochlear implantation with a guide tube. *Int J Comput Assist Radiol Surg* 2016;11(S1):1–286.